Andrzej NOWAK[1], Paweł NOWAK[1], Mirosław KURZ[2], Czesław RYGUŁA[2]

University of Bielsko-Biała, Department of Computer Modelling (1), ESP Division in Pszczyna, RAFAKO S.A. (2)

Study of the effect of the stiffness of the anvil beam for vibration propagation in the system of collecting electrodes

*Streszczenie. W artykule przedstawiono eksperymentalnie zweryfikowany model dyskretny układu elektrod zbiorczych elektrofiltru suchego. Do modelowania układu zastosowano metodę sztywnych elementów skończonych (SES). Celem symulacji było poszukiwanie rozwiązań optymalnych sztywności drąga strzepującego ze względu na maksymalne amplitudy drgań oraz ich zrównoważony rozkład w układzie elektrod zbiorczych. (**Badanie wpływu sztywności drąga strzepującego na propagację drgań w układzie elektrod zbiorczych**).*

Abstract. The paper presents experimentally verified computational model of the collecting electrodes in ESP. Discretisation of the whole system is carried out by means of the modified rigid finite element method (RFEM). The aim of the simulations is to find correlation between stiffness of an anvil beam and vibration propagation, which guaranties the maximum amplitudes of vibrations and their proper distribution in the plates. The results of the conducted analyses may be useful to engineers and designers of ESP.

Słowa kluczowe: elektrody zbiorcze, SES, analiza drgań, weryfikacja eksperymentalna.
Keywords: collecting electrodes, RFEM, vibration analysis, experimental verification.

Introduction

The effectiveness of electrostatic precipitators (ESP) depends on many factors, like: charging of particles (ionization), transporting the charged particles to the collecting surfaces (migration), precipitation of the charged particles onto the collecting surfaces (collection), neutralizing the charged particles on the collecting surfaces (charge dissipation), removing the particles from the collecting surface to the hopper (particle dislodging) and, finally, conveying the particles from the hopper to a disposal point (particle removal). Presented research are concerned only with one of those phenomena which is the particle dislodging. In the case of ESP with a gravitational system of rappers, the removal of the particulate matter collected on the electrodes (plates) occurs as a result of excitation of vibrations of accelerations allowing for the effective removal of particles coagulated on their surfaces. The analysis of the phenomena accompanying the operation of rapping devices, the improvement of reliability of the operation of rapping systems and the achievement of more efficient removal of particulates from collecting electrodes have been under investigation for many years [1, 2]. Initially, the studies were based on physical models [3], however, in the last decade, instead of building physical models of ESP, specialized, numerically advanced models are created, which serve to perform simulations of a whole device [4] or only its selected subassemblies [5].

The paper presents experimentally verified computational model of the collecting electrodes in ESP. Discretisation of the whole system, both the beams and the electrodes, is carried out by means of the modified rigid finite element method (RFEM). The RFEM allows easy to reflect mass and geometrical features of the considered. Moreover, the method is convenient for the introduction of additional concentrated masses which reflects elements such as the joints that fasten the electrodes to the suspension beam (top beam), an anvil beam (bottom beam), distance-marking bushes, riveted or screw joints, etc... The system of nine electrodes 16 m long and several various stiffness of an anvil beam in this system are analyzed. The aim of the simulations is to find correlation between stiffness of an anvil beam and vibration propagation, which guaranties the maximum amplitudes of vibrations and their proper distribution in the plates.

The earlier works of the authors [6], [7] present models allowing for a simulation of vibrations of electrodes, induced by an impulse force. In the above mentioned publications much space is devoted to the validation of the models – by comparing the results of measurements and computer simulations. The adopted compatibility criteria demonstrated that practically all the applied methods give a satisfactory consistency of the results in the range of peak values of accelerations. It also applies to the RFEM, used in the current study.

Based on the models verified with the use of measurements, an attempt was made to use the developed computer software to determine the effect of geometric and structural parameters of the electrode-rapper system on the values of accelerations. The results of the conducted analyses may be useful to engineers and designers of ESP.

RFEM model

The test system comprises 9 plates of collecting electrodes (E1, E2,…, E9), of a length $L = 16$ m, made of sheet metal of a thickness $h = 1,5$ mm, hanging on a common suspension beam (SB) and fastened at the bottom by an anvil beam (AB), terminated with an anvil (A) on the side of the anvil beam (Fig. 1).
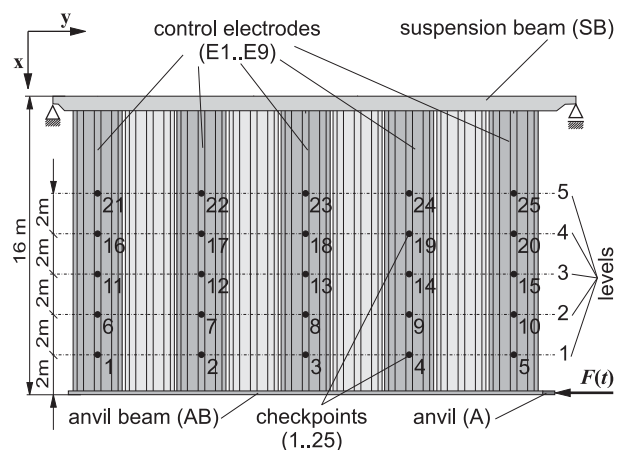

Fig.1. The system of collecting electrodes

In the rapping system a beater, having a weight $m = 8$ kg was mounted. The course of the impulse force $F(t)$ generated by the beater is shown in figure 2. The model reflects configuration which is typical for the current designs in the industry.
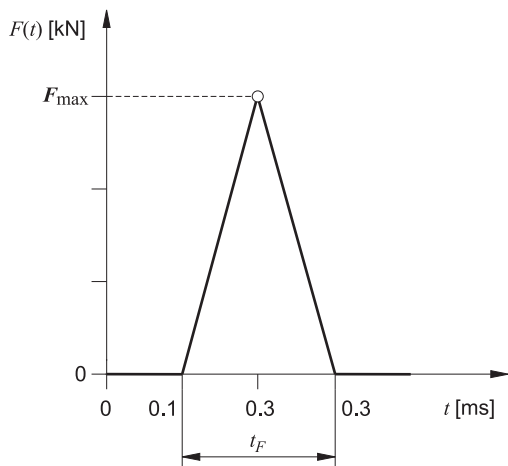
Fig.2. The course of the impulse force $F(t)$

Numerical simulation enabled us to analyse the influence of stiffness of an anvil beam on vibration propagation in the system. It was assumed 5 of control levels, spaced themselves every 2 m. At each level accelerations were computed in 5 checkpoints (Fig. 1). In the studies related to simulation of vibrations in collecting electrodes of dry electrostatic precipitators, it is necessary to correctly determine the course of impact force of a beater on an anvil beam to which the plates with deposited particulate matter are attached. Knowledge of the course of the impulse force $F(t)$ is necessary to determine the load

in the modelled system of collecting electrodes. Moreover, the courses of these forces have a direct impact on the effectiveness of rapping particulate matter, and therefore on accelerations causing the detachment of dust particles. In previous work the authors presented a procedure, which allows for an approximate determination of the course of impact force, based on the results of vibration measurements and computer simulation, in which a self-developed model of the system was used [8].

As already mentioned, previous studies of the authors present models and algorithms allowing for the analysis of vibrations of collecting electrodes using different methods. Papers [6], [7] present a model obtained by the finite element method, paper [6] describes a model using the plate strip method, while in paper [7] a model obtained using a so-called hybrid method is presented. In all these studies the rigid finite element method was used to discretise the beams. Further, a validation of these models, comparing the results of calculations with the results of the measurements and using the Abaqus commercial package was performed. The RFEM was also used for modelling the vibrations of the plates of electrostatic precipitators and the results of model validation and software based on this method were as satisfactory as in case of using the aforementioned methods of discretisation of plates. Currently RFEM method is also used for modelling of dynamics of risers during vessel motion [9]. In the present work we use the RFEM for the discretisation of the system as it is shown in figure 3.
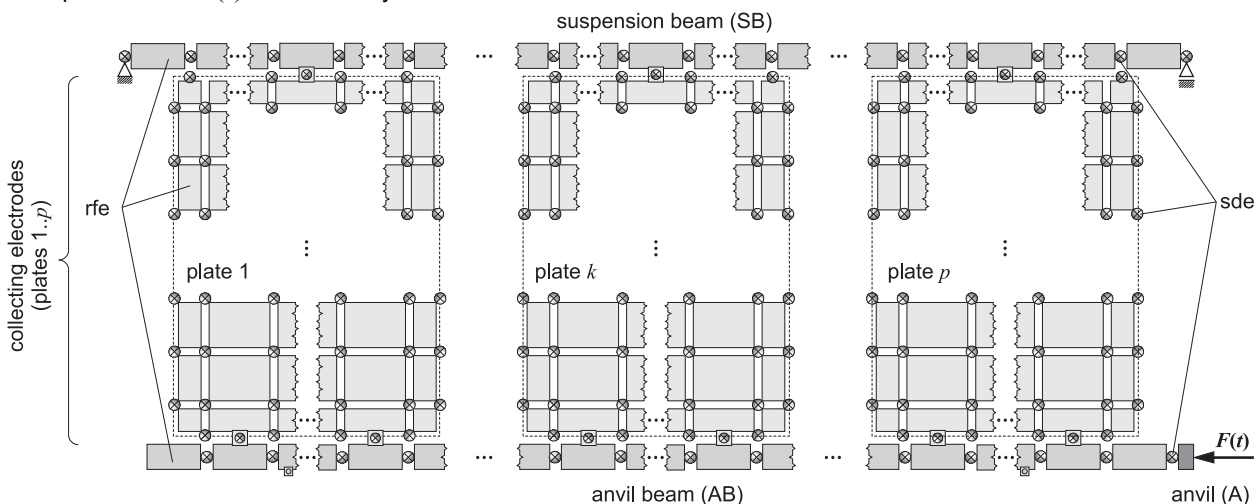

Fig.3. Diagram of a system discretized using the RFEM method: rfe – rigid finite element, sde – spring-damping element

The equation of motion of the discretized system can be expressed as a system of ordinary second-order differential linear equations in the form:

(1) $$\mathbf{M\ddot{q}} + \mathbf{Kq} = \mathbf{f} ,$$

where: $\mathbf{M}$ – diagonal mass matrix, $\mathbf{K}$ – stiffness matrix of constant coefficients, $\mathbf{f} = \mathbf{f}(\mathbf{F}(t))$ – input vector,

$$\mathbf{q} = \left[\mathbf{q}_1^{\,T}, ..., \mathbf{q}_i^{\,T}, ..., \mathbf{q}_n^{\,T} \right]^T , \quad \mathbf{q}_i = \left[x_i, y_i, z_i, \varphi_i, \theta_i, \psi_i \right]^T ,$$

x_i, y_i, z_i – coordinates of the centre of rfe mass, $\varphi_i, \theta_i, \psi_i$ – small angles of rfe rotations.

$\mathbf{M}$ and $\mathbf{K}$ matrices are matrices with constant coefficients. The advantage of the RFE method is a diagonal matrix $\mathbf{M}$. The integration of equations (1) was performed using the Newmark method with a constant integration step.
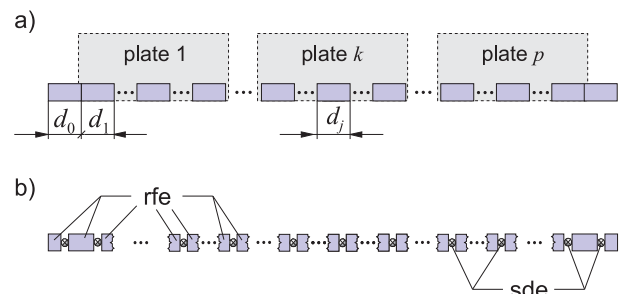

Fig.4. Division of beams into rfe and sde: a) primary, b) secondary

In the RFE method the flexible body (beam) is divided into rigid elements reflecting inertial features of the body (Fig. 4a). Then, during the secondary division, massless and non-dimensional spring-damping elements (sde) representing bending features with length d_j are placed in the middle of the rigid elements (Fig. 4b). Stiffness matrix

$\mathbf{K}$ of a primary element can be presented in the general form:

$$(2) \qquad \mathbf{K} = \mathbf{D}^T \cdot \mathbf{C} \cdot \mathbf{D} ,$$

where: $\mathbf{C}$ – stiffness matrix of sde, $\mathbf{D}$ – matrix of coefficients of constrain equations.

In this work it is assumed that matrix K is:

$$(3) \qquad \mathbf{K} = f\left(c_x, c_y, c_z, c_\varphi, c_\theta, c_\psi\right).$$

When the linear physical relations describe the characteristic of the discretized links, stiffness coefficients are calculated according to the formulas:

$$(4) \qquad c_x = \frac{12EI_z}{\left(d_j\right)^3} ,$$

$$(5) \qquad c_y = \frac{EA}{d_j} ,$$

$$(6) \qquad c_z = \frac{12EI_x}{\left(d_j\right)^3} ,$$

$$(7) \qquad c_\varphi = \frac{EI_x}{d_j} ,$$

$$(8) \qquad c_\theta = \frac{GI_y}{d_j} ,$$

$$(9) \qquad c_\psi = \frac{EI_z}{d_j} ,$$

where: E – Young's modulus of elasticity, G – shear modulus, A – cross-section area, I_x, I_y, I_z – inertial moments of the cross-section area.

c_y is longitudinal stiffness coefficient, c_x and c_z are shear stiffness coefficients, c_θ is torsional stiffness coefficient, c_φ and c_ψ are bending stiffness coefficients. Various values of these coefficients were obtained by changing value and shape of the cross-section of the beam.

Simulations – numerical calculations

It is assumed that the value of the impulse force will change linearly (Fig. 2) – increase from zero to a certain value F_{max}, and then linearly decrease to zero within a predetermined time interval t_F. Based on the test results obtained from one of the manufacturer of electrostatic precipitators it was assumed that $t_F = 0,0002$ s and $F_{max} = 100$ kN.

The analysis of the influence of the stiffness of the anvil beam onto the propagation of vibrations in the system are performed for two types of beam cross-section: prismatic and circular (Fig. 5).

The study of the influence of the stiffness of the anvil beam for vibration propagation in the system of collecting electrodes was limited to the analysis of cases presented in table 1.
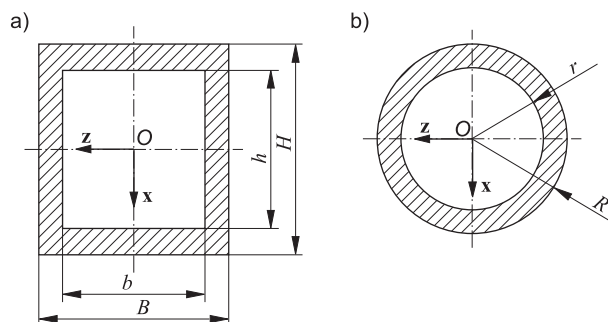

Fig.5. Cross-section of the anvil beam: a) cross-section prismatic, b) cross-section circular

Table 1. Dimensions of cross-section of the anvil beam

Cross-section prismatic							
k	B [mm]	H [mm]	b [mm]	H [mm]	A_p [m²] x10⁻³	I_x [m⁴] x10⁶	I_y [m⁴] x10⁶
p1	80	70	0	0	5,600	2,987	2,287
p2	80	70	16	6	5,504	2,985	2,286
p3	80	70	32	22	4,896	2,927	2,258
p4	80	70	48	38	3,776	2,636	2,067
p5	80	70	64	54	2,144	1,807	1,447
p6	80	70	72	62	1,136	1,058	0,857
p7	80	40	64	24	1,664	1,182	0,353
p8	40	80	24	64	1,664	0,353	1,182
p9	60	60	44	44	1,664	0,768	0,768
p10	60	60	0	0	3,600	1,080	1,080
p11	60	60	12	12	3,456	1,078	1,078
p12	60	60	24	24	3,024	1,052	1,052
p13	60	60	36	36	2,304	0,940	0,940
p14	60	60	48	48	1,296	0,638	0,638
p15	60	60	54	54	0,684	0,371	0,371
p16	80	80	64	64	2,304	2,015	2,015
p17	70	70	54	54	1,984	1,292	1,292
p18	50	50	34	34	1,344	0,409	0,409
p19	40	40	24	24	1,024	0,186	0,186
p20	30	30	14	14	0,704	0,064	0,064
Cross-section circular							
k	R [mm]		r [mm]		A_p [m²] x10⁻³	I_x [m⁴] x10⁶	I_y [m⁴] x10⁶
o1	37		29		1,664	0,925	0,925
o2	40		0		5,027	2,011	2,011
o3	40		8		4,825	2,007	2,007
o4	40		16		4,222	1,959	1,959
o5	40		24		3,217	1,750	1,750
o6	40		32		1,810	1,187	1,187
o7	40		36		0,955	0,691	0,691
o8	50		42		2,312	2,465	2,465
o9	45		37		2,061	1,749	1,749
o10	35		27		1,558	0,761	0,761
o11	30		22		1,307	0,452	0,452

Vibrations of electrodes have a nature of high-frequency processes. However, a direct comparison of such courses is not very effective. For this reason, the present study compares peak values, median of peak values and A_s^k – coefficient of even distribution of peak values throughout the system. These values are expressed by the following dependencies:

$$(10) \qquad W_{s,i,\max}^k = \max_{0 \le t \le T} \left| a_{s,i}^k \right| ,$$

$$(11) \qquad Me_s^k = \underset{i=1..n}{median}\left(W_{s,i,\max}^k\right) ,$$

$$(12) \qquad A_s^k = \max_{i=1..n}\left(W_{s,i,\max}^k\right) - \min_{i=1..n}\left(W_{s,i,\max}^k\right) ,$$

$$A_s^{k,l} = Me_s^k - \min_{i=1..25}\left(W_{s,i,\max}^k\right), \tag{13}$$

$$A_s^{k,u} = \max_{i=1..25}\left(W_{s,i,\max}^k\right) - Me_s^k, \tag{14}$$

where: T – time of the analysis, k – index of cross-section variant (Table 1), i – index of the control point, n – number of checkpoints ($n = 25$).

In the above equations it was assumed that $a_{s,i}^k$ can be one of the following values:

$$a_{s,i}^k = \begin{cases} a_{x,i}^k & \text{– acceleration in the direction of axis } \mathbf{x}, \\ a_{y,i}^k & \text{– acceleration in the direction of axis } \mathbf{y}, \\ a_{t,i}^k = \sqrt{a_{x,i}^2 + a_{y,i}^2} & \text{– tangential acceleration in plane } \mathbf{xy}, \\ a_{n,i}^k = a_{z,i} & \text{– normal acceleration in plane } \mathbf{xy}, \\ a_{c,i}^k = \sqrt{a_{x,i}^2 + a_{y,i}^2 + a_{z,i}^2} & \text{– total acceleration}, \end{cases}$$

therefore $s = \{x,y,t,n,c\}$.
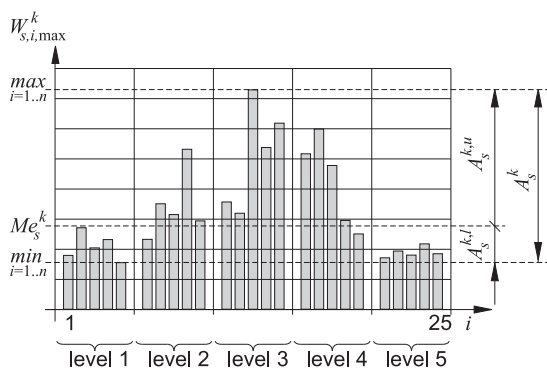
Fig.6. The physical interpretation of formulas (10-14)

Results and discusion

The influence of the wall thickness of the prismatic profile (exterior dimensions: 70x80 mm) onto the propagation of vibrations in the collecting electrode system is shown in figure 7.
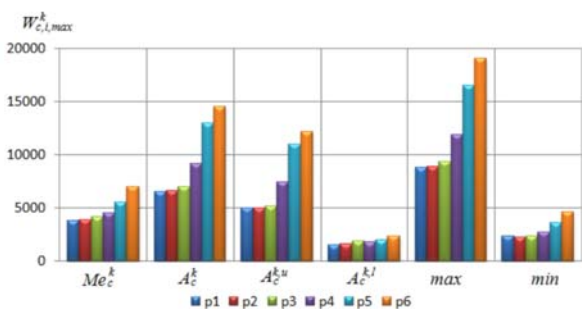

Fig.7. The influence of the wall thickness of the prismatic profile (exterior dimensions: 70x80 mm) onto total acceleration

The influence of the exterior dimensions of the prismatic and circular profile (while cross-section area is constant and wall thickness equals 8 mm) onto the propagation of vibrations in the collecting electrode system is shown in figures 8 and 9.
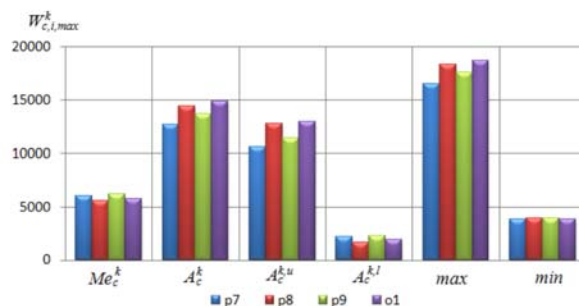

Fig.8. The influence of the exterior dimensions of the prismatic and circular profile onto total acceleration
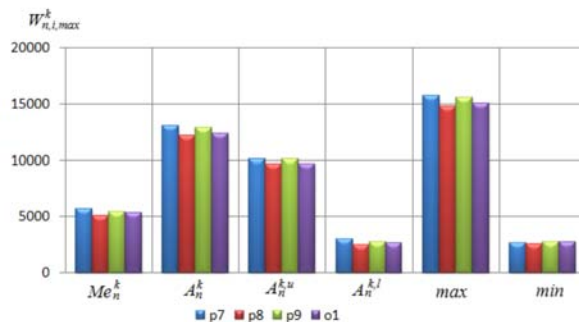

Fig.9. The influence of the exterior dimensions of the prismatic and circular profile onto normal acceleration

The influence of the wall thickness of the prismatic profile (exterior dimensions: 60x60 mm) onto the propagation of vibrations in the collecting electrode system is shown in figure 10.
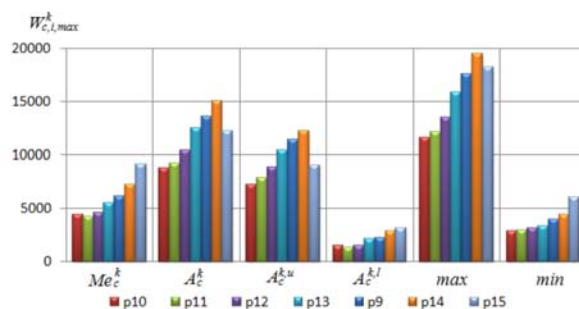

Fig.10. The influence of the wall thickness of the prismatic profile (60x60 mm)

The influence of the exterior dimensions of the prismatic profile (while wall thickness is constant and equals 8 mm) onto the propagation of vibrations in the collecting electrode system is shown in figures 11 and 12.
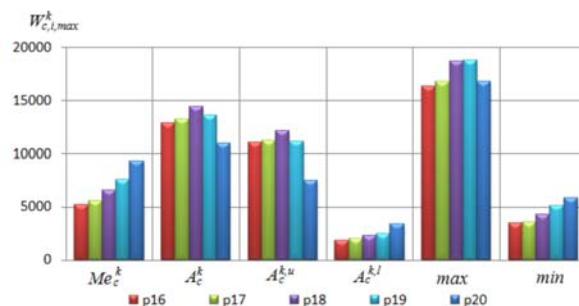

Fig.11. The influence of the exterior dimensions of the prismatic profile (constant wall thickness 8 mm) onto total acceleration
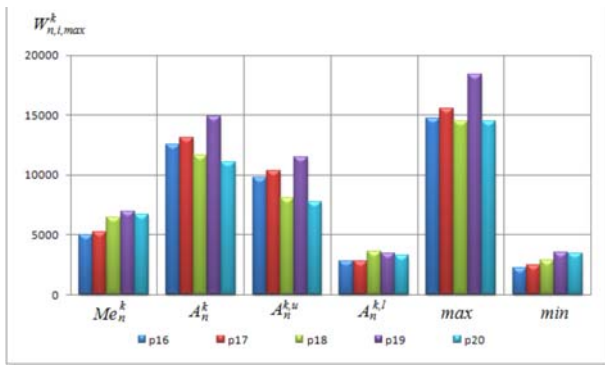
Fig.12. The influence of the exterior dimensions of the prismatic profile (constant wall thickness 8 mm) onto normal acceleration

The influence of the wall thickness of the circular profile (exterior radius R is constant) onto the propagation of vibrations in the collecting electrode system is shown in figure 13.
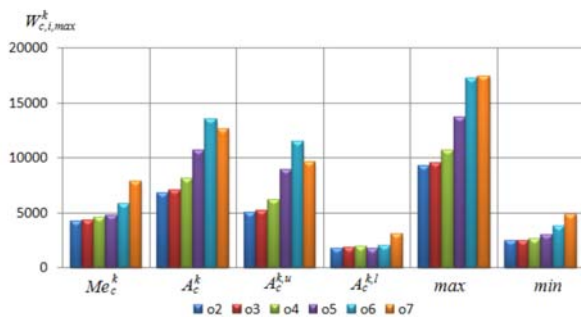

Fig.13. The influence of the wall thickness of the circular profile (exterior radius R is constant)

The influence of the exterior radius R of the circular profile (while wall thickness is constant and equals 8 mm) onto the propagation of vibrations in the collecting electrode system is shown in figure 14.
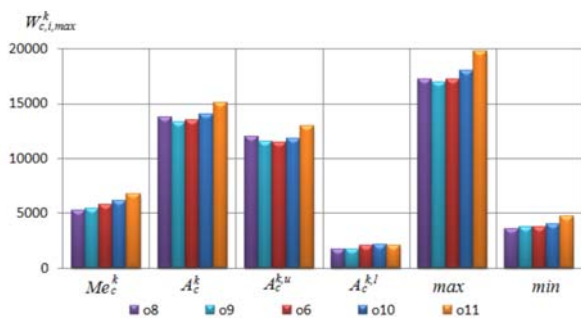

Fig.14. The influence of the exterior radius R of the circular profile (constant wall thickness 8mm).

The experiments presented in the present study imply the following remarks:

1. The values of total acceleration cannot only determine the selection of a profile of anvil beam - we should check all the components of acceleration, specially values of normal acceleration as an important factor for the particle dislodging (Fig. 8,9,11,12).

2. The values of one of the factors presented in formulas 10-14 cannot also determine the selection of a profile of anvil beam. Only analysis of all of factors allows for the selection optimal variant of the anvil beam's profile.

3. As it is shown in the present study (Fig. 7, 10 and 13) the best values of presented factors of propagation of vibrations in the collecting electrodes system (high values of $median$ and min, small values of A and $A^{k,l}$) are generated for profiles with thinner walls. However, it should be noted that too small wall thickness of the profile could be a reason of destruction of the collecting electrodes system.

4. As shown in figures 11 and 14 profiles with smaller cross-section area generated better results on the size and distribution of vibrations.

Authors: dr hab. inż. Andrzej Nowak, prof. ATH, Akademia Techniczno-Humanistyczna w Bielsku-Białej, Katedra Modelowania Komputerowego, ul. Willowa 2, 43-309 Bielsko-Biała, E-mail: a.nowak@ath.bielsko.pl; mgr inż. Paweł Nowak, Akademia Techniczno-Humanistyczna w Bielsku-Białej, Katedra Modelowania Komputerowego, ul. Willowa 2, 43-309 Bielsko-Biała, E-mail: pnowak@ath.bielsko.pl; dr inż. Mirosław Kurz, „RAFAKO" S.A. w Raciborzu, RAFAKO S.A., ul. Łąkowa 33, 47-400 Racibórz, E-mail: miroslaw.kurz@rafako.com.pl; mgr inż. Czesław Ryguła, „RAFAKO" S.A. w Raciborzu, RAFAKO S.A., ul. Łąkowa 33, 47-400 Racibórz, E-mail: Czeslaw.Rygula@rafako.com.pl

REFERENCES
[1] Talaie M.R., Journal of Hazardous Materials, 124 (2005), 1–3, 44–52
[2] Yang, X.F., Kang, Y.M., Zhong, K., Journal of Hazardous Materials, 169 (2009), 1–3, 941–947
[3] Lee, J.–K., Ku, J.–H., Lee, J.–E., Kim, S.–C., Ahn, Y.–C., Shin, J.–H., Choung, S.–H., in Proc. ICESP VII, Kyongju, Korea, September 20–25, (1998)
[4] Francis S.L., Bäck, A., Johansson, P., in Proc. ICESP XI, Hangzhou, China, October 20–25 (2008), 45–49
[5] Caraman N., Bacchiega G., Gallimberti I., Arrondel V., Hamlil M., in Proc. ICESP X, , 2006, Cairns, Australia, Jun. 25–29 (2006)
[6] Adamiec-Wójcik I., Nowak A., Wojciech S., Acta Mech. Sinica 1 (2011), 27, 72–79
[7] Adamiec-Wójcik I., Awrejcewicz J., Nowak A.,Wojciech S., Mathematical Problems in Engineering, (2014). Article ID 832918, 19 pages, doi:10.1155/2014/832918
[8] Nowak A., Nowak P., Wojciech S., in Proc. 13th International Conference on Dynamical Systems - Theory and Applications, Łódź, Poland, December 7–10 (2015)
[9] Adamiec-Wójcik I., Brzozowska L., Drąg Ł., Ocean Engineering, 106 (2015), 102–114